DOI: 10.1002/ejic.200900089

Modulation of Photochemical Properties in Ion-Controlled Multicomponent Dynamic Devices

Mihail Barboiu,*[a,b] Yves-Marie Legrand,[b] Luca Prodi,*[c] Marco Montalti,[c] Nelsi Zaccheroni,[c] Gavin Vaughan,[d] Arie van der Lee,[b] Eddy Petit,[b] and Jean-Marie Lehn*[a]

Keywords: Fluorescence / Molecular devices / Structural switching / Metallosupramolecular complexes / Terpyridine / Zinc

A bis-pyrenyl-terpyridine ligand **1** has been synthesised and used to prepare zinc homo- and heterocomplexes and their photophysical properties have been studied. Fluorescence titrations displayed modulation of absorption and emission, depending on the molarities of the ionic species (Zn^{2+}, H^+). Two single-crystal structures give insights into the formation of multicomponent supramolecular networks, also present in solution as shown by NMR and ESI-MS spectroscopy. NMR spectroscopy revealed fast exchanges of the ligands complexed around the metal ion, which could be reduced at lower temperature. Conformational (from W to U shape) and photophysical changes of the flexible ligand were demonstrated in the solid and liquid phases. Addition of zinc ions to the solution of ligands changes the absorption and fluorescence spectra noticeably. The zinc complexes do not form exciplexes; the fluorescence is mainly due to charge-transfer transitions. The present work illustrates the potential use of ion-triggered switches to generate mechanical motions that can be followed photophysically.

Introduction

The control of molecular motion in photoactive assemblies is of interest for understanding the energy and electron-transfer processes occurring in biological systems. It may also be useful in the fabrication of supramolecular photonic devices for energy conversion and storage.[1] Mechano-devices effecting triggered molecular motions induced by light excitation, electron transfer[2] or ion binding[3] provide the basis for controlled, dynamic structural changes based on rotations and translations or coiling/uncoiling processes. Nanomechanical devices may involve shape modification between two (or more) forms presenting different photochemical properties, substrate recognition/binding or release processes controlled by external stimuli that induce a motional/mechanical shape switch.[4]

Multicomponent arrays based on metallosupramolecular complexes are the focus of extensive investigation.[5]

Those involving rack systems and especially those containing multimetallic centres[6] are highly attractive because of their photophysical and redox properties, which enable such systems to behave as "molecular wires".[7] Examples studied so far that involve linear arrangements of organic chromophores aligned along a molecular wire scaffold are relatively rare. In particular, incorporating multiple ligands that can adapt their geometrical features along a multivalent bridge in a donor-bridge/acceptor-ligands scaffold is attractive. Indeed, the host–guest interactions between the vicinal multiple chromophoric sites may be mediated by the bridge, which can control the electronic coupling of the donor (D) and the acceptor (A) groups, as is usually observed in the natural photosynthetic system.[8]

In this context, we have recently reported the modulation of photoluminescence properties in a motional process involving the reversible switching between a highly luminescent ligand **1** in a W-shaped state and its poorly luminescent metallosupramolecular U-shaped complex **2**, triggered by ion complexation/decomplexation reactions (Scheme 1).[3a]

In complex **2**, the ligand **1** presents a wrapped U-shaped conformation, which has the two pyrene moieties positioned in face-to-face arrangement. This provides a slot suitable for the intercalation of a terpyridine unit (terpy) **3**, coordinated to the Zn^{2+} cation and leading to the formation of a π-donor/π-acceptor/π-donor triad, which presents a considerable overlap between aromatic groups. Recent studies of related systems involve tuning of electronic coupling in chromophore-appended terpyridines by ion complex-

[a] Laboratoire de Chimie Supramoléculaire, ISIS, Université Louis Pasteur,
8, allée Gaspard Monge, BP 70028, 67083 Strasbourg, France
Fax: +33-3-90-24-51-40
E-mail: lehn@isis.u-strasbg.fr
[b] Institut Européen des Membranes, IEM-CNRS 5635,
Place Eugène Bataillon, CC 47, 34095 Montpellier, France
E-mail: barboiu@iemm.univ-montp2.fr
[c] Università di Bologna, Dipartimento di Chimica "G. Ciamician",
Via Selmi 2, 40126 Bologna, Italy
E-mail: lprodi@ciam.unibo.it
[d] European Synchrotron Radiation Facility, ESRF,
BP 220, 38043 Grenoble, France

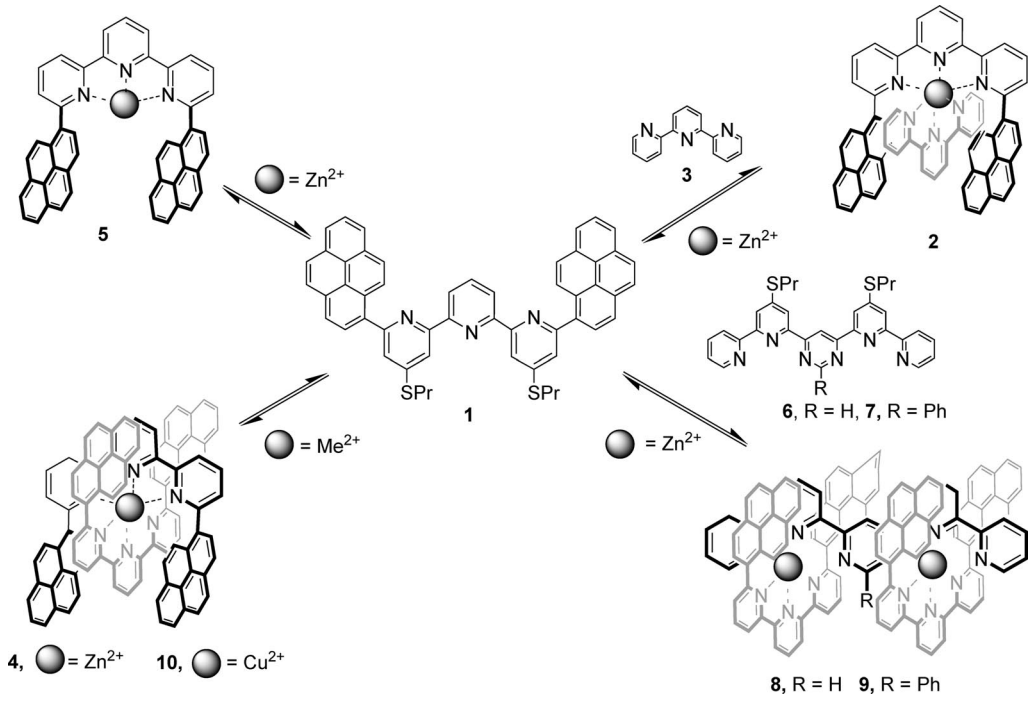

Scheme 1. Synthetic scheme for preparation of multicomponent dynamic devices. The S*n*Pr substituents of ligands were omitted for clarity.

ation as well as tweezer-type binding processes.[9] As a continuation of these studies on dynamic chemical devices,[3] we describe herein the ionic modulation of new photoactive devices based on α,α′-pyrene terpy derivative **1**. This ligand is capable of a butterfly-type molecular motion triggered by metal ion binding and self-associating in homoduplex **4** (or **10**) as well as in multichromophoric site rack-type complexes **8** and **9**. In the latter case, the two units of U-shaped Zn^{2+} complexes of **1** are aligned along bis-terpy-type oligoheterocyclic strands **6** and **7** consisting of alternating pyridine (py) and pyrimidine (pym) subunits connected in α,α′ positions.

Results and Discussion

Ion-Driven Self-Assembly of Ligand 1 in Solution

The synthesis of ligand **1** has already been described.[3c] This α,α′-pyrene terpy derivative **1**, discussed in this paper, operates under conditions in which the available terpyridine (terpy) coordination sites can be involved in the orthogonal binding events of the octahedral metal ions. The conversion of the bis-terminally pyrene-appended compound **1** into the corresponding metal complex transforms an unwrapped free ligand into a wrapped compact coordination complex. In such complexes of ligand **1**, the two terminal α,α′-linked π-donor pyrene units are situated in a face-to-face arrangement, suitable for (i) the insertion of a flat aromatic π-acceptor, such as a terpy-like unit in complex **2**,[3c] or (ii) insertion of a self-inserted unit of **1** in complex **4**, yielding a compact π–π stacking subset of three overlapping aromatic rings.

^{1}H NMR titrations were performed on solutions of $Zn(CF_3SO_3)_2$ and **1** in [D_3]acetonitrile. Initial complexation studies revealed that addition of $Zn(CF_3SO_3)_2$ to the [D_3]-acetonitrile suspensions of **1** caused a rapid dissolution of the ligand in a Zn^{2+}/**1** molar ratio from 0.5:1 to 2:1. All the titration steps showed very complex broad-signal ^{1}H NMR spectra at 25 °C, indicative of the presence of exchanging species in solution. At 268 K the spectra display essentially sharp signals for ligand **1** located in different magnetic environments (Figure 1), consistent with slow interconversion between complexes **4**, $[\mathbf{1}_2Zn]^{2+}$, and **5**, $[\mathbf{1}Zn]^{2+}$, and with the presence of two isomers for each complex of parallel and of antiparallel orientation of the pyrene moieties in complexes **5** and **6** (see ref.[3a] for details).

In the homoduplex complex **4**, $[\mathbf{1}_2Zn]^{2+}$, the aromatic proton signals were overall shielded by 3.0 ppm with respect to ligand **1** (Figure 1). The pyrenyl substituents are spatially close to the terpyridine centre and play an important role in the aggregation process of these compounds in solution. An important upfield shielding is still present in the spectrum of **5**, $[\mathbf{1}Zn]^{2+}$, indicative of exchanging equilibria in solution with homoduplex **4**, $[\mathbf{1}_2Zn]^{2+}$. For this reason, ESI-MS spectrometry was used to follow the titration of an acetonitrile solution of **1** by a solution of $Zn(CF_3SO_3)_2$ (Figure 2) in order to obtain information about the coordination behaviour of **1** towards Zn^{2+} ions. The addition of $Zn(CF_3SO_3)_2$ to an acetonitrile suspension of **1** caused the total dissolution of the ligand only at a **1**/Zn^{2+} molar ratio of 1:0.5. At a ratio of **1**/M^{2+} of 1:0.5, the ESI mass spectrum was consistent with the presence of the $[\mathbf{1}_2Zn]^{2+}$ **4** complex (*m*/*z* = 814.5, 100%) (Figure 2). Further addition of Zn^{2+} ions led to the progressive conversion of **5** into the

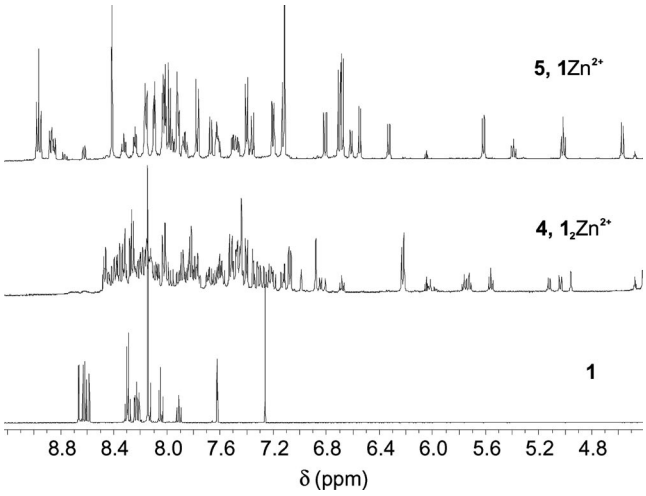

Figure 1. ^{1}H NMR spectra at 268 K in [D_3]acetonitrile of ligand **1**, complex **4**, $[\mathbf{1}_2Zn]^{2+}$, and complex **5**, $[\mathbf{1}Zn]^{2+}$, respectively.

$[\mathbf{1}Zn]^{2+}$ **5** complex (*m*/*z* = 463.8 and 514, 72.6% (mol/mol) at the **1**/Zn^{2+} ratio of 1:1 and 84.6% (mol/mol) at the **1**/Zn^{2+} ratio of 1/2).

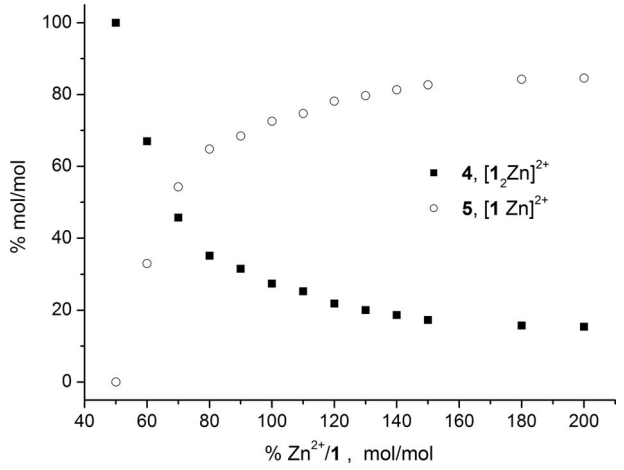

Figure 2. Distribution curves of the complexes **5** (■) and **6** (○) resulted in the titration of a solution of ligand **1** in CH_3CN by a solution of Zn^{2+} ion in CH_3CN (at initial ligand **1** concentration of 0.001 M). The data points were plotted using the integral surface of characteristic MS-chromatogram peaks obtained from ESI mass spectra.

Solid-State Structure of the Homoduplex Complex 10

Layering an acetonitrile solution of **1**/$Zn(CF_3SO_3)_2$ (2:1 and 1:1, mol/mol) with isopropyl ether (5:1, v/v) resulted in the formation of yellow crystals, which were investigated by X-ray crystallography. Despite their favourable aspect, only poor crystals could be obtained, but nonusable data could be collected even using a high-intensity synchrotron X-ray source. Fortunately, by layering an acetonitrile solution of **1**/$Cu(CF_3SO_3)_2$ (2:1, mol/mol) with isopropyl ether (5:1, v/v), crystals suitable for X-ray analysis were obtained. We can consider that the complexes **4** $[\mathbf{1}_2Zn](CF_3SO_3)_2$ and **10** $[\mathbf{1}_2Cu](CF_3SO_3)_2$ are isostructural: self-complementary homoduplex complexes which self-assemble in the solid state as intriguing architectures, resulting from the multiple π–π stacking and CH–π interactions of the pyrene substituents.

The unit cell of **10** $[\mathbf{1}_2Cu](CF_3SO_3)_2$ was found to contain two $[\mathbf{1}_2Cu^{2+}]$ complexes, together with four triflate counterions and four isopropyl ether molecules. The molecular and the crystal packing structures of **10** are presented in Figure 3. In the structure, two ligands **1** and one Cu^{2+} ion form a duplex. The copper cations presenting an octahedral geometry are coordinated by two terpy units of the ligand **1** (the average Cu^{2+}–N distance is 2.28 Å). In complex **10** the ligand **1** presents two different wrapped U-shaped conformations: one has the two pyrene substituents relatively positioned in a face-to-face (parallel) arrangement and the other one in an antiparallel conformation (Figure 3, a), confirming the ^{1}H NMR results. It provides for each molecule a slot suitable for the intercalation of a terpy unit of ligand **1** coordinated to the Cu^{2+} cation, leading to the formation of two π-donor/π-acceptor/π-donor triads, presenting a considerable overlap between aromatic groups with an average centroid–centroid distance of 3.50 Å.

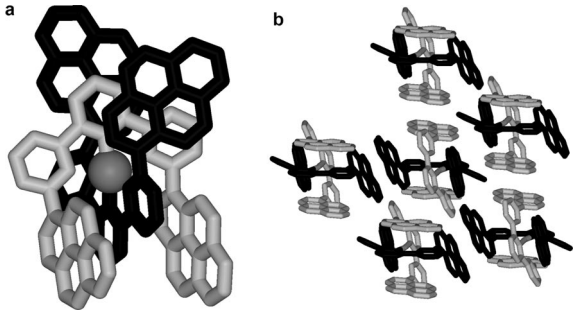

Figure 3. Crystal structure of complex **10** $[\mathbf{1}_2Cu](CF_3SO_3)_2$: (a) stick representation; (b) representation of the arrangements of the entities in the crystal; the *n*PrS substituents and H atoms have been omitted for clarity.

In the crystal structure, the duplex **10** presents a tight contact with the four neighbouring ones by taking advantage of three π–π stacking interactions of the two pyrene side arms of two different molecules (average distance of 3.90 Å) and four CH–π interactions between one pyrene moiety and two pyrene side arms emanating from two different neighbouring molecules (average distance = CH–pyrene plane of 2.80 Å) (Figure 3, b). The anions and solvent molecules fill the interstices between the complex cations.

Synthesis of Rack-Type Complexes 8 and 9

Addition of **1**/$Zn(CF_3SO_3)_2$ mixtures (1:1 mol/mol) to acetonitrile suspensions of ligands **6** or **7**[10] caused a rapid dissolution of the ligands to give red solutions of the complexes **8** $[\mathbf{1}_2\mathbf{6}Zn_2](CF_3SO_3)_4$ and **9** $[\mathbf{1}_2\mathbf{7}Zn_2](CF_3SO_3)_4$, respectively. They showed a very complex and ^{1}H NMR spectrum with broad signals at 25 °C, indicative of the pres-

ence of several exchanging species in solution. ESI mass spectra of the acetonitrile solutions of **8** and **9** were consistent with the presence of the $[\mathbf{1}_2Zn_2\mathbf{6}]^{4+}$ (m/z = 557.7, 80%), $[\mathbf{1}Zn\mathbf{3}]^{2+}$ (m/z = 691.9, 40%), $[\mathbf{1}_2Zn_2\mathbf{6}Tf]^{3+}$ (m/z = 793.50, 20%) and respectively $[\mathbf{1}_2Zn_2\mathbf{7}]^{2+}$ (m/z = 633.7, 80%), $[\mathbf{1}Zn\mathbf{7}]^{2+}$ (m/z = 767.9), $[\mathbf{1}_2Zn_2\mathbf{7}Tf]^{3+}$ (m/z = 869.50, 60%) species in solution.

Solid-State Structure of Rack-Type Complex 9

Layering a solution of complex **9** $[\mathbf{1}_2\mathbf{7}Zn_2](CF_3SO_3)_4$ (yield 100%) in acetonitrile with isopropyl ether (5:1, v/v) resulted in the formation of only red crystals of **9** that were investigated by X-ray crystallography. Despite their favourable aspect, only a partially resolved crystal structure of **9** was obtained. The data collected using a high-intensity synchroton X-ray source are representative of a severe disorder among the triflate anions, acetonitrile solvent molecules and terminal ligand *n*PrS moieties, precluding the successful refinement of the structure. The complex $[\mathbf{1}_2\mathbf{7}Zn_2]$ was, however, relatively stable against data refinement.

The unit cell of **9** was found to contain four $[\mathbf{1}_2\mathbf{7}Zn_2]$ entities, together with triflate counterions and isopropyl ether solvent molecules. The well-resolved structure of the complex cation $[\mathbf{1}_2\mathbf{7}Zn_2]$ demonstrates the connectivity in agreement with the two-rack-type structure, resulting from self-assembly of two ligands **1** and two Zn^{2+} ions together with one ligand **7** (Figure 4). In complex **9**, the Zn^{2+} ions display distorted octahedral coordination geometry. The average Zn–N distances are 2.30 Å for both pyridine and pyrimidine nitrogen atoms. The two ligand **1** molecules are crystallographically nonequivalent, consistent with the presence of similar parallel and antiparallel relative orientations of the pyrene moieties in the complex. The four pyrene π-donor moieties provide a double slot suitable for the intercalation of a two-site π-acceptor ligand **7** coordinated to the Zn^{2+} cation, leading to a considerable overlap between aromatic groups with an average centroid–centroid distance of 3.50 Å. The terpy unit of the ligand **1** presents a slight deviation from planarity but in complex **9** these moieties are almost parallel (average distance of 7.1 Å) and perpendicular to the plane of the two-site ligand **7**. The phenyl ring orthogonal to the plane of the ligand **7** is intercalated between the terpy units, also indicating strong π–π stacking interactions (Figure 4, a).

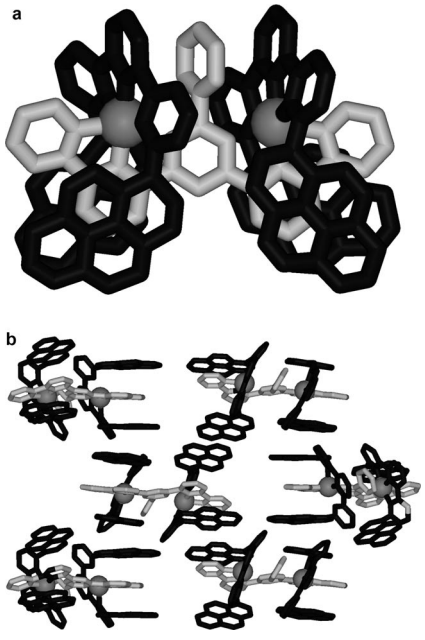

Figure 4. Crystal structure of complex **9** $[\mathbf{1}_2Zn_2\mathbf{7}](CF_3SO_3)_4$: (a) stick representation; (b) representation of the arrangements of the entities in the crystal; the *n*PrS substituents and H atoms have been omitted for clarity.

In the crystal lattice the complex cations **9** pack into parallel layers that are alternately stratified above each other in an ABAB arrangement. One molecule of complex **9** presents tight contact with the four neighbouring ones by taking advantage of four π–π stacking interactions (Figure 4, b) of the four pyrene side arms (average distance of 3.90 Å). The anions and solvent molecules fill the interstices between the complex cations.

Photophysical Properties of Complexes 2, 4, 5, 8 and 9

The most relevant photophysical data of the ligand **1** and complexes **2**, **4**, **5**, **8** and **9** are gathered in Table 1, while the absorption spectra in dichloromethane solution are shown in Figure 5.

Table 1. Photophysical properties of ligand **1** and of its complexes **2**, **4**, **5**, **8** and **9** at room temperature.

	λ_{max} [nm]	ε_{max} [$M^{-1}\,cm^{-1}$]	λ_{max} [nm]	Φ	Solvent
1[a]	348	59200	404	0.33	CH_2Cl_2
	348	62500	401	0.34	$CHCl_3/CH_3CN$
4	342	125400	550	$<5\times10^{-5}$	CH_2Cl_2
	341	128000	565	$<5\times10^{-5}$	CH_3CN
5	342	69100	575	$<5\times10^{-5}$	CH_2Cl_2
	342	71400	589	$<5\times10^{-5}$	CH_3CN
2	340	70200	527	$<5\times10^{-5}$	CH_2Cl_2
	341	71100	573	$<5\times10^{-5}$	CH_3CN
8	341	121000	591	$<5\times10^{-5}$	CH_2Cl_2
	341	123200	608	$<5\times10^{-5}$	CH_3CN
9	341	119600	563	$<5\times10^{-5}$	CH_2Cl_2
	341	121500	537	$<5\times10^{-5}$	CH_3CN

[a] The lifetime of τ = 2.6 ns is similar in both solvent systems.

It must be underlined that complexation with d^{10} Zn^{2+} ions does not usually introduce low-energy metal-centred or charge-transfer states, so that MC, MLCT or LMCT bands are not expected to be present in the absorption spectrum of these complexes. As a consequence, the absorption spectra should be regarded as the sum of the transitions involving the ligands present in the different species, perturbed by metal ion complexation[11] and π-stacking interactions among them. In the 320–400 nm region, all the complexes behave very similarly, both in acetonitrile and in dichloromethane solution. In particular, the pyrene-centred band laying in this spectral region experiences a blueshift at its maximum, but with a noticeable increase of the ab-

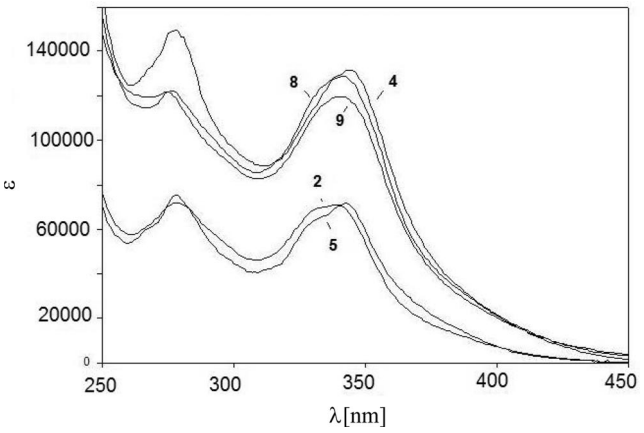

Figure 5. Room temperature absorption spectra of the complexes **2**, **4**, **5**, **8** and **9** in CH_2Cl_2.

sorption tail in the red part of the spectrum. The overall effect can be explained by taking into account two different phenomena. The first one is due to the complexation of the ligand with the metal ion, which decreases the electronic density on the terpy moiety and, as a consequence, perturbs the delocalisation of the electronic density to the pyrene unit, leading to the observed blueshift of the band. Moreover, this process makes the terpy unit easier to be reduced, so that a charge-transfer transition from the pyrene (E_{ox} = +1.18 V vs. SCE in acetonitrile)[11c,11d] becomes possible. In addition, as can be clearly observed in the X-ray structures, metal ion complexation brings the two pyrene moieties of **1** and the terpy-type unit of the second ligand **1**, **3**, **6** or **7** in close proximity, so that π-stacking interactions between those three units can be established. Interactions of this kind are expected to cause a broadening of the bands of the chromophore involved, as indeed observed. This argument is not valid for complex **5**, which, in fact, presents the least pronounced tail of all the complexes studied in this work. As far as complex **5** is concerned, however, it is noted that the absorption in the 370–420 nm region depends on the solvent as it is more pronounced in dichloromethane. This finding supports the attribution of this band to a charge-transfer transition, in agreement with earlier discussions.[3c]

All five complexes examined, both in dichloromethane and in acetonitrile solutions, show a very weak ($\Phi < 5 \times 10^{-5}$), large and unstructured fluorescence band in the 480–750 nm region. The excitation spectra, again in all cases, are proportional to the absorption ones. In acetonitrile solution, the typical band of ligand **1** can also be observed. However, in the spectra of the complexes, this band shows a reduced intensity (<2% with respect to that of the free ligand) and, at the same time, an unquenched excited-state lifetime as well as a corrected excitation spectrum that is proportional to that of the ligand. These findings are a clear indication that such a signal is due to the small portion of the ligand that, in this solvent, is dissociated according to the equilibrium discussed below. In dichloromethane, where the association is stronger, the contribution of this band is almost negligible. The fluorescence band of the complexes can in theory be attributed, because of its shape, energy and solvent dependency, to: (i) a charge-transfer transition, from the pyrene moiety to the coordinated terpy unit, (ii) the formation of intramolecular excimers (involving the two pyrene chromophore of the same ligand) or (iii) the formation of exciplexes (involving the pyrene chromophores of one ligand and the terpy moiety of a second ligand). This latter term is clearly absent in **5**, where, however, a large fluorescence band is still observed, while the typical excimer fluorescence from a couple of pyrene chromophores lies at much higher energies. These arguments strongly support the attribution of such a band to a charge-transfer transition.

Fluorescence Titration Experiments of 1

Because of the presence of different complexation equilibria between **1** and metal ions, it appeared of interest to perform titration experiments in $CHCl_3/CH_3CN$ solutions with Zn^{2+} and H^+ ions. As expected from the already discussed photophysical properties of **4** and **5**, the addition of Zn^{2+} ions to a solution of **1** leads to noticeable changes in the absorption (Figure 6, a) and fluorescence (Figure 6, b) spectra. From the analysis of the absorption and emission

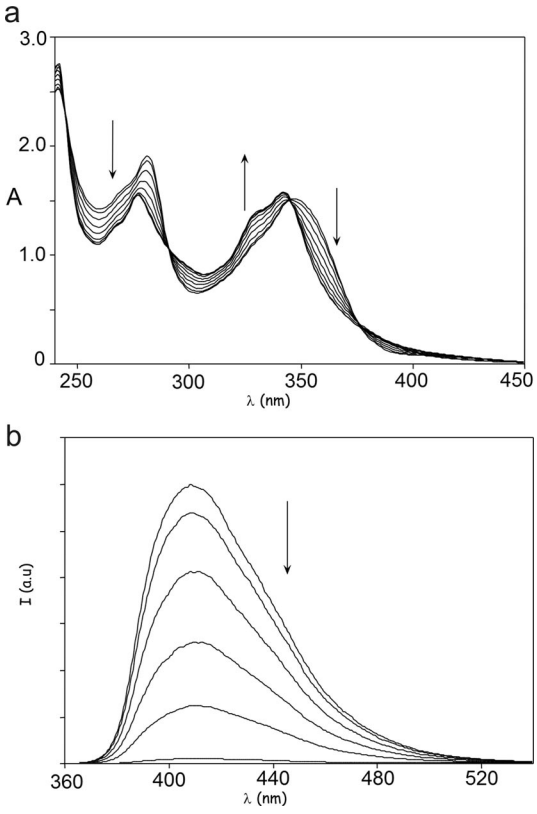

Figure 6. (a) Absorption spectra in $CHCl_3/CH_3CN$ (v/v, 1:1) and (b) room temperature fluorescence spectra (λ_{exc} 290 nm, isosbestic point) in $CHCl_3/CH_3CN$ (v/v, 1:1) of **1** and upon addition of increasing amounts of $Zn(ClO_4)_2$.

spectra taken during the titration experiments, the following cumulative association constants could be obtained for the different equilibria (1) and (2).

$$Zn^{2+} + \mathbf{1} \rightleftharpoons \mathbf{5}^{2+} \log \beta_{11} = 8.0 \pm 0.3 \quad (1)$$

$$Zn^{2+} + 2^*\mathbf{1} \rightleftharpoons \mathbf{4}^{2+} \log \beta_{12} = 14.6 \pm 0.5 \quad (2)$$

According to the above-proposed model, which supports the formation of the two complexes **4** and **5** also in solution, the calculated absorption and fluorescence spectra of the species formed can be obtained and are shown in Figure 7, parts a and b, respectively. As can be seen from the comparison of Figures 5, 6 and 7 and from the data collected in Table 1, the spectra are very similar to those observed when directly dissolving the relative complexes.

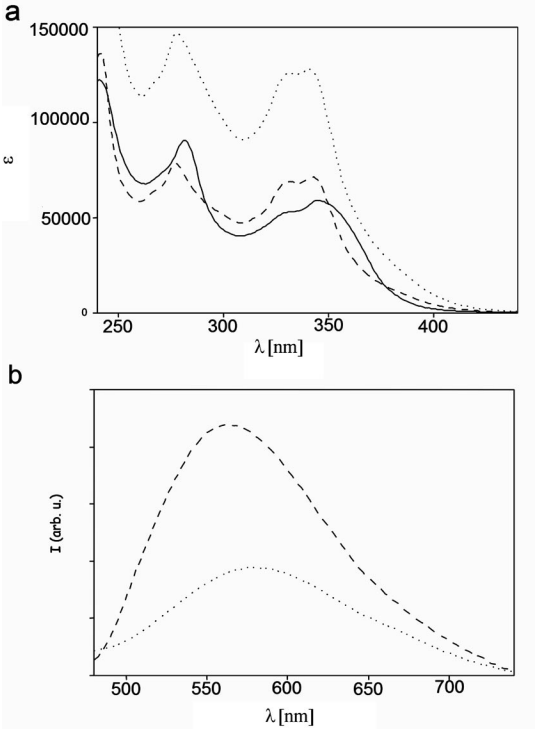

Figure 7. (a) Calculated absorption spectra of the species formed during the titration of **1** with $Zn(ClO_4)_2$ in $CHCl_3/CH_3CN$ (v/v, 1:1): **1** (−), **4** (·····) and **5** (- - - - -); (b) calculated fluorescence spectra (λ_{exc} 290 nm, isosbestic point) of the species formed during the titration of **1** with $Zn(ClO_4)_2$ in $CHCl_3/CH_3CN$ (v/v, 1:1): **4** (- - - -) and **5** (·····).

Interestingly, addition of triflic acid leads to qualitatively similar results. In particular with a blueshift of the absorption band at 341 nm an increase of the absorption in the 380–500 nm region could be observed (Figure 8). This was accompanied by a complete quenching of the fluorescence band of the ligand already after the addition of half an equivalent, and the appearance, at the end, of a large weak band with a λ_{max} at 618 nm. This suggests that the protonation of **1** led to the U-shaped conformation of the ligand. Moreover, the addition of half an equivalent of acid resulted in the formation of a dimeric complex like in **4**, probably self-associated through H bonds between pyridine/protonated pyridine groups. Then, the addition of 1 equiv. of acid resulted in the formation of the monoprotonated monomeric complex, like in **5**. These findings support the conclusion that photophysical changes observed during the formation of the different zinc complexes do not directly involve the metal ion, whose main effect is to change the electronic density of the ligand upon coordination.

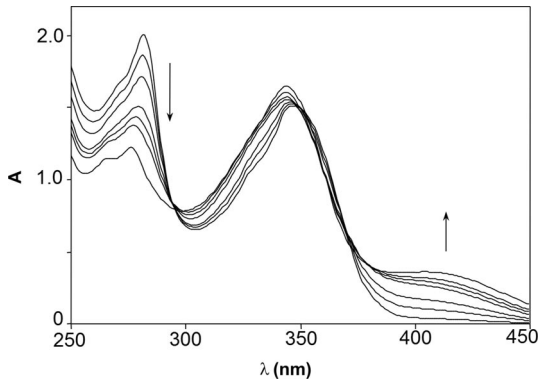

Figure 8. Absorption spectra in $CHCl_3/CH_3CN$ of **1** and upon addition of increasing amounts of triflic acid.

Conclusions

The present results illustrate the design, synthesis and photophysical properties of three conformational switches, displaying extension–compression motions on metal-ion coordination, accompanied by a continuous change of their optical properties. The bistable pyrene-terpyridine-pyrene-based receptor **1** converts from a W to a U shape upon ion-metal cation complexation. The U form of **1** is capable of substrate binding through insertion between the lateral donor-pyrene arms of acceptor-terpyridine-type systems, with the participation of the metal ions simultaneously coordinating the binding units of such multicomponent dynamic devices. The coupling of ionically triggered changes in the shape of the ligand **1** with the quenching of the fluorescence of the pyrene fluorophore previously observed in complex **2**[3c] is consistent with the energy transfer between the pyrene and terpyridine units, in homoduplex complex **4** as well as in heteroduplex rack-type complexes **8** and **9**. Further attempts to synthesise larger ligands are currently in progress to extend this work toward nanoscale molecular optical wires.

Experimental Section

General Methods: Compound **1** was prepared according to procedures described in the literature.[3a] All reagents were obtained from commercial suppliers and used without further purification. THF was distilled from benzophenone/Na. All organic solutions were routinely dried using sodium sulfate (Na_2SO_4). The solvents used for the photophysical measurements were acetonitrile and dichloromethane from Merck (UVASOL). Column chromatography was carried out on Merck alumina activity II–III. ^1H NMR, ^{13}C NMR, COSY and NOESY spectra and NMR ionic modula-

tion experiments were recorded with a 250 MHz Bruker spectrometer with samples dissolved in $CDCl_3$, NO_2CD_3 or CD_3CN, with the use of the residual solvent peak as reference. Mass spectrometric studies were performed in the positive-ion mode using a quadrupole mass spectrometer (Micromass, Platform II). Samples were dissolved in acetonitrile and were continuously introduced into the mass spectrometer through a Waters 616HPLC pump (flow rate of 10 mL min^{-1}). The temperature (60 °C) and the extraction cone voltage (V_c = 5–10 V) were usually set to avoid fragmentations. The microanalyses were carried out at Service de Microanalyses, Institut Charles Sadron, Strasbourg.

Photophysical Studies: UV/Vis absorption spectra were obtained by using a Perkin–Elmer Lambda 16 spectrophotometer. Uncorrected emission and corrected excitation spectra were obtained with a Perkin–Elmer LS 50 spectrofluorimeter. The fluorescence lifetimes (uncertainty ±5%) were obtained with an Edinburgh single-photon counting apparatus, in which the flash lamp was filled with D_2. Luminescence quantum yields (uncertainty ±15%) were determined using quinine sulfate in 0.5 M H_2SO_4 aqueous solution (F = 0.546).

X-ray Diffraction Experiments for 9 and 10: Red single crystals of $C_{160}H_{136}F_{12}N_{16}O_{13}S_{10}Zn_2$ (**9**) were grown from acetonitrile and yellow single crystals of $C_{112}H_{84}Cu_1F_6N_8O_6S_6$ (**10**) from an acetonitrile/isopropyl ether mixture. X-ray diffraction data measurements for **9** were collected at 173 K and were carried out at beamline ID11 at the European Synchrotron Facility (ESRF) at Grenoble. A wavelength of 0.32826 Å was selected using a double crystal Si(111) monochromator. Single-crystal data for **10** were collected at 173 K using a Gemini four-circle diffractometer (Oxford-Diffraction) with graphite-monochromated Mo-K_α radiation. ω-scans were used in all cases. The structure was solved using the ab initio charge flipping method with the Superflip program[12a] and refined using the CRYSTALS software.[12b] The H atoms were all located in a difference map, but repositioned geometrically by initially refining them with soft restraints on the bond lengths and angles to regularise their geometry and U_{iso}(H) (in the range 1.2–1.5 times U_{eq} of the parent atom), after which the positions were refined with riding constraints. The structure of **10** appeared to contain much disorder in the solvent and counterions, but contrary to the disorder in the structure of **9**, this could be reasonably well modelled.

Basic structural data for **9** and **10** are as follows. **9**: a = 18.3166(17) Å, b = 40.2845(30) Å, c = 21.0461(19) Å, α = 90°, β = 103.652(4)°, γ = 90°, V = 15090.6(1) Å^3, space group $P2_1/c$. **10**: a = 16.3788(2) Å, b = 17.9072(3) Å, c = 19.1840(3) Å, α = 111.7143(17)°, β = 109.9913(14)°, γ = 90.7414(12)°, V = 4849.35(15) Å^3, space group $P\bar{1}$, 179036 reflections measured, 12461 independent reflections with $I > 2\sigma(I)$ used for refinement with 1114 parameters; R = 0.128. wR = 0.141.

CCDC-714171 contains the supplementary crystallographic data for **10**. These data can be obtained free of charge from The Cambridge Crystallographic Data Centre via www.ccdc.cam.ac.uk/data_request/cif.

Acknowledgments

This work, conducted as part of the award "Dynamic Adaptive Materials for Separation and Sensing Microsystems" (M. B.) made under the European Heads of Research Councils and European Science Foundation EURYI (European Young Investigator) Awards Scheme in 2004, was supported by funds from the Participating Organizations of EURYI and the EC Sixth Framework Program (see www.esf.org/euryi). This work was also supported by ANR-Blanc Programme-POLYFUNMAG.

[1] a) J.-M. Lehn, *Supramolecular Chemistry – Concepts and Perspectives*, VCH, Weinheim, **1995**, chapter 8; b) J.-M. Lehn, *Proc. Natl. Acad. Sci. USA* **2002**, *99*, 4763–4768; c) J.-M. Lehn, in: *Supramolecular Science: Where It Is and Where It Is Going* (Eds.: R. Ungaro, E. Dalcanale), Kluwer, Dordrecht, **1999**, pp. 287–304.

[2] a) V. Balzani, F. Credi, M. Raymo, J. F. Stoddart, *Angew. Chem.* **2000**, *112*, 3484–3530; *Angew. Chem. Int. Ed.* **2000**, *39*, 3348–3391; b) Molecular Machines Special Issue, *Acc. Chem. Res.* **2001**, *34*, issue 6; c) S. Shinkai, T. Nakaji, T. Ogawa, K. Shigematsu, O. Manabe, *J. Am. Chem. Soc.* **1981**, *103*, 111–115.

[3] a) M. Barboiu, J.-M. Lehn, *Proc. Natl. Acad. Sci. USA* **2002**, *99*, 5201–5206; b) M. Barboiu, G. Vaughan, N. Kyritsakas, J.-M. Lehn, *Chem. Eur. J.* **2003**, *9*, 763–769; c) M. Barboiu, L. Prodi, M. Montalti, N. Zaccheroni, N. Kyritsakas, J.-M. Lehn, *Chem. Eur. J.* **2004**, *10*, 2953–2959; d) M. Linke-Schaetzel, C. E. Anson, A. K. Powell, G. Buth, E. Palomares, J. D. Durrant, T. S. Balaban, J.-M. Lehn, *Chem. Eur. J.* **2006**, *12*, 1931–1940; e) A. Petitjean, F. Puntoriero, S. Campagna, A. Juris, J.-M. Lehn, *Eur. J. Inorg. Chem.* **2006**, *19*, 3878–3892; f) A. Petitjean, R. G. Khoury, N. Kyritsakas, J.-M. Lehn, *J. Am. Chem. Soc.* **2004**, *126*, 6637–6647.

[4] a) B. Feringa (Ed.), *Molecular Switches*, Wiley-VCH, Weinheim, **2001**; b) V. Balzani, A. Credi, M. Venturi, *Molecular Devices and Machines*, Wiley-VCH, Weinheim, **2003**.

[5] a) B. H. Northrop, H. B. Yang, P. J. Stang, *Chem. Commun.* **2008**, 5896–5908; b) C. D. Meyer, C. S. Joiner, J. F. Stoddart, *Chem. Soc. Rev.* **2007**, *36*, 1705–1723; c) S. Leininger, B. Olenyuk, P. J. Stang, *Chem. Rev.* **2000**, *100*, 853–908; d) G. F. Swiegers, T. F. Malfetese, *Chem. Rev.* **2000**, *100*, 3483–3538; e) S. R. Seidel, P. J. Stang, *Acc. Chem. Res.* **2002**, *35*, 972–983; f) M. Fujita, K. Umemoto, M. Yoshizawa, N. Fujita, T. Kusukawa, K. Biradha, *Chem. Commun.* **2001**, 509–518; g) M. Ruben, J. Rojo, F. J. Romero-Salguero, L. H. Uppadine, J.-M. Lehn, *Angew. Chem.* **2004**, *116*, 3728–3747; *Angew. Chem. Int. Ed.* **2004**, *43*, 3644–3662.

[6] a) G. S. Hanan, C. Arana, J.-M. Lehn, D. Fenske, *Angew. Chem.* **1995**, *107*, 1191–1193; *Angew. Chem. Int. Ed. Engl.* **1995**, *34*, 1122–1124; b) G. S. Hanan, C. Arana, J.-M. Lehn, G. Baum, D. Fenske, *Chem. Eur. J.* **1996**, *2*, 1292–1302; c) A.-M. Stadler, F. Puntoriero, S. Campagna, N. Kyritsakas, R. Welter, J.-M. Lehn, *Chem. Eur. J.* **2005**, *11*, 3997–4009; d) F. Loiseau, F. Nastasi, A.-M. Stadler, S. Campagna, J.-M. Lehn, *Angew. Chem.* **2007**, *119*, 6256–6259; *Angew. Chem. Int. Ed.* **2007**, *46*, 6144–6147.

[7] a) Molecular Wires: From Design to Perspectives: L. De Cola (Ed.), *Top. Curr. Chem.* **2005**, *257*; b) J. L. Segura, N. Martin, D. M. Guldi, *Chem. Soc. Rev.* **2005**, *34*, 31–47.

[8] R. E. Blankenship, *Molecular Mechanisms of Photosynthesis*, Blackwell, Oxford, **2002**.

[9] a) A. Harriman, A. Khatyr, R. Ziessel, *Dalton Trans.* **2003**, 2061–2068; b) T. Moriuchi, M. T. Nishiyama, T. Hirao, *Eur. J. Inorg. Chem.* **2002**, 447–451; c) Y. M. Legrand, A. van der Lee, M. Barboiu, *Inorg. Chem.* **2007**, *46*, 9083–9089; d) M. Büschel, M. Helldobler, J. Daub, *Chem. Commun.* **2002**, 1338–1339; e) J. P. Schneider, J. W. Kelly, *J. Am. Chem. Soc.* **1995**, *117*, 2533–2546; f) P. B. Glover, P. R. Ashton, L. J. Childs, A. Rodger, M. Kercher, R. M. Williams, L. De Cola, Z. Pikramenou, *J. Am. Chem. Soc.* **2003**, *125*, 9918–9919; g) H. M. Colquhoun, Z. Zhu, D. J. Williams, *Org. Lett.* **2003**, *5*, 4353–4356; h) M. Barboiu, E. Petit, G. Vaughan, *Chem. Eur. J.* **2004**, *10*, 2263–2270; i) M. Barboiu, J.-M. Lehn, *Rev. Chim.* **2006**, *57(9)*, 909–914; j) M. Barboiu, J. M. Lehn, *Rev. Chim.* **2008**, *i59*, 255–259; k) F. Dumitru, E. Petit, A. van der Lee, M. Barboiu, *Eur. J. Inorg. Chem.* **2005**, *21*, 4255–4262; l) M. Barboiu, E. Petit, A. van der Lee, G. Vaughan, *Inorg. Chem.* **2006**, *45*, 484–486.

[10] a) G. S. Hanan, U. S. Schubert, D. Volkmer, E. Rivière, J.-M. Lehn, N. Kyritsakas, J. Fischer, *Can. J. Chem.* **1997**, *75*, 169–182; b) D. M. Bassani, J.-M. Lehn, G. Baum, D. Fenske, *Angew. Chem.* **1997**, *109*, 1931–1933; *Angew. Chem. Int. Ed. Engl.* **1997**, *36*, 1845–1847; c) M. Barboiu, J.-M. Lehn, *Rev. Roum. Chim.* **2006**, *51*, 581–588.

[11] a) L. Prodi, *New J. Chem.* **2005**, *29*, 20–31; b) L. Prodi, M. Montalti, N. Zaccheroni, G. Pickaert, L. Charbonnière, R. Ziessel, *New J. Chem.* **2003**, *27*, 134–139; c) F. Loiseau, C. Di Pietro, S. Serroni, S. Campagna, A. Licciardello, A. Manfredi, G. Pozzi, S. Quici, *Inorg. Chem.* **2001**, *40*, 6901–6908; d) L. Prodi, R. Ballardini, M. T. Gandolfi, R. Roversi, *J. Photochem. Photobiol., A* **2000**, *136*, 49; e) A. Credi, V. Balzani, S. Campagna, G. S. Hanan, C. R. Arana, J.-M. Lehn, *Chem. Phys. Lett.* **1995**, *243*, 102.

[12] a) L. Palatinus, G. Chapuis, *J. Appl. Crystallogr.* **2007**, *40*, 786–790; b) P. W. Betteridge, J. R. Carruthers, R. I. Cooper, K. Prout, D. J. Watkin, *J. Appl. Crystallogr.* **2003**, *36*, 1487.

Received: January 23, 2009
Published Onliine: May 7, 2009

